

See discussions, stats, and author profiles for this publication at: <https://www.researchgate.net/publication/242015868>

# Comparison Effects and Dielectric Properties of Different Dose Methylene-Blue-Doped Hydrogels

ARTICLE *in* THE JOURNAL OF PHYSICAL CHEMISTRY B · JUNE 2013

Impact Factor: 3.3 · DOI: 10.1021/jp402219t · Source: PubMed

---

CITATIONS

5

---

READS

112

## 4 AUTHORS, INCLUDING:



Orhan Yalçın

Niğde Üniversitesi

53 PUBLICATIONS 256 CITATIONS

SEE PROFILE

# Comparison Effects and Dielectric Properties of Different Dose Methylene-Blue-Doped Hydrogels

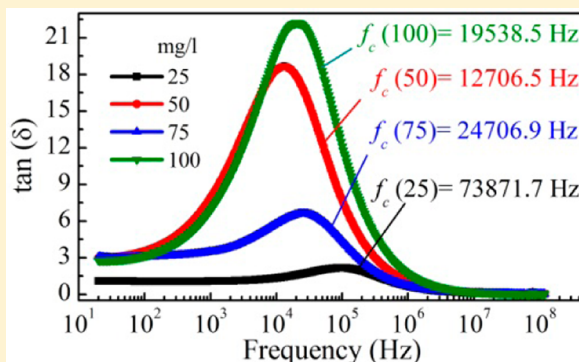
O. Yalçın,\*<sup>†</sup> R. Coşkun,<sup>§</sup> M. Okutan,<sup>||</sup> and M. Öztürk<sup>‡</sup>

<sup>†</sup>Department of Physics and <sup>‡</sup>Institute of Graduate School of Natural and Applied Sciences, Niğde University, 51240, Niğde, Turkey

<sup>§</sup>Department of Chemistry, Bozok University, 66500 Yozgat, Turkey

<sup>||</sup>Department of Physics, Yıldız Technical University, 34210 Istanbul, Turkey

**ABSTRACT:** The dielectric properties of methylene blue (MB)-doped hydrogels were investigated by impedance spectroscopy. The real part ( $\epsilon'$ ) and the imaginary part ( $\epsilon''$ ) of the complex dielectric constant and the energy loss tangent/dissipation factor ( $\tan \delta$ ) were measured in the frequency range of 10 Hz to 100 MHz at room temperature for pH 5.5 value. Frequency variations of the resistance, the reactance, and the impedance of the samples have also been investigated. The dielectric permittivity of the MB-doped hydrogels is sensitive to ionic conduction and electrode polarization in low frequency. Furthermore, the dielectric behavior in high-frequency parts was attributed to the Brownian motion of the hydrogen bonds. The ionic conduction for MB-doped samples was prevented for Cole–Cole plots, while the Cole–Cole plots for pure sample show equivalent electrical circuit. The alternative current (ac) conductivity increases with the increasing MB concentration and the frequency.



## 1. INTRODUCTION

Currently, pure and doped hydrogels are receiving a great deal of interest as a class of 3D structures of hydrophilic polymers networks.<sup>1,2</sup> Hydrogels are frequently utilized in chemistry, biology, drug delivery/pharmaceutical, biomedicine, sanitary pads, food, tissue engineering, biocompatibility, wound dressing, agriculture, dental materials, implants, injectable polymeric systems, ophthalmic applications, hybrid-type organs, photoelectronics, biosensors, some ecological problems, engineered tissue scaffolds, ultrahigh power density capacitors, and so on.<sup>3–38</sup> Hydrogels are being produced using a variety of methods, including swelling of cross-linked structures in an aqueous medium such as water or alcohols like methanol, ethanol, or benzyl alcohol, which are characterized using various techniques.<sup>14,22–25,39–47</sup> Some metal, dextran, organic plasticizer, montmorillonite, graphene-containing hydrogels are considered as a new generation of elastic materials with a range of potential applications as biocompatible polymers,<sup>48–52</sup> liquid crystals,<sup>53,54</sup> smart materials,<sup>55,56</sup> and Cu-ion-doped hydrogels.<sup>2</sup> Hydrogels are classified into two groups as physical-gel/reversible and chemical-gel/permanent.<sup>57,58</sup> Mechanical, magnetic, optical, electrical, physical, and chemical properties of functionalized hydrogels were investigated in the literature.<sup>59–96</sup> However, dielectric properties of methylene blue (MB)-doped hydrogels have not been previously reported. In addition, there is no detailed information about the impedance, resistance and reactance of MB-doped hydrogels in the literature. The dielectric properties of pure, transition-metal ions and MB-doped hydrogels were investigated using the

impedance spectroscopy (IS) over the frequency range of 10 Hz to 100 MHz.

We have studied the MB concentration effects and dielectric properties of MB-doped hydrogels by using dielectric spectroscopy (DS or IS). The frequency evolution of the real part ( $\epsilon'$ ) and the imaginary part ( $\epsilon''$ ) of the complex dielectric constant and energy loss factor of MB-doped hydrogels were studied in the 10 Hz to 100 MHz frequency range. In particular, frequency-dependent resistance, reactance, and impedance values for MB-doped hydrogels were analyzed at room temperature (RT). The main purpose of this study is to investigate the dielectric properties of ionic hydrogels containing ionic groups such as MB dopants and the effects varying MB concentration. Dielectric properties of MB-doped hydrogels are also affected by the ionic interactions between loaded polymers and free ions.

## 2. EXPERIMENTAL DETAILS

**2.1. Sample Preparation and MB Loading Study.** The hydrogels, poly (2-acrylamido-2-methylpropane sulfonic acid-*co*-itaconic acid (poly(AMPS-*co*-IA)), were synthesized by copolymerization of AMPS and IA in aqueous medium using *N,N'*-methylenebisacrylamide (MBAAm) as cross-linker and potassium persulfate (KPS) as initiator. (See, for detail, refs 2, 97, and 98.) The chemical formulation of the hydrogels and

**Received:** March 4, 2013

**Revised:** June 18, 2013

**Published:** June 25, 2013



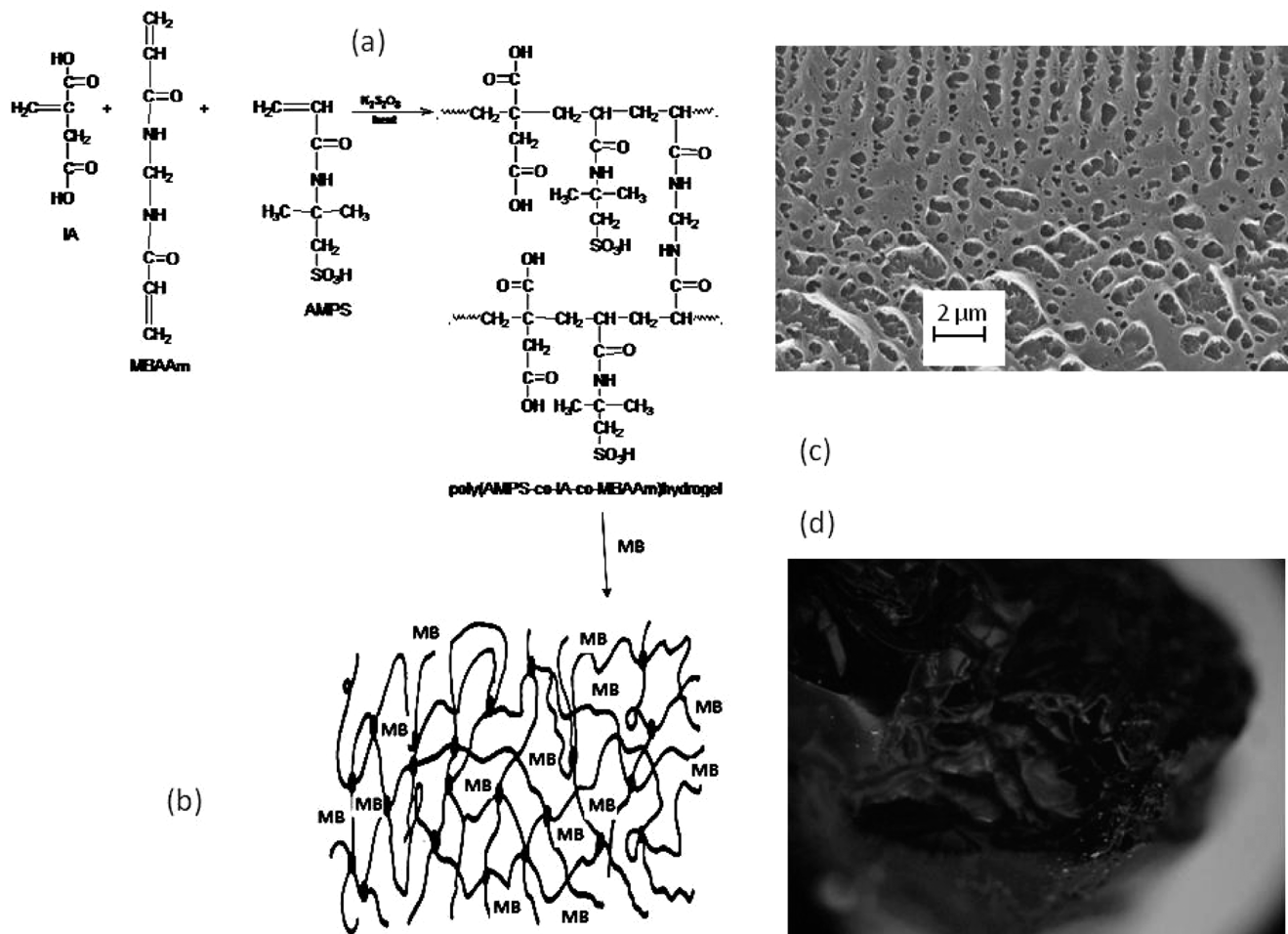


**Figure 1.** (a) Structure/chemical formulation of pure poly(AMPS-co-IA) hydrogels. (b) Schematic representation of the hydrogels doped with MB. (c) SEM images of pure hydrogels. (d) Light microscopy (400 $\times$ ) images of 50 mg/L doped with MB.

scanning electron microscopy (SEM) image are shown in Figure 1a,c, respectively. We added 0.1 g hydrogels to model solutions in a 100 mL Erlenmeyer that included pH-adjusted 30 cm<sup>3</sup> MB solution with various concentrations (25, 50, 75, and 100 mg/L). The mixtures were shaken with a shaker for 24 h at 25 °C. The MB-loaded hydrogels were taken from the Erlenmeyer and were washed with deionized water and dried in an oven at 55 °C. The schematic representations of MB-doped hydrogels and their light microscopy images are seen in Figure 1b,d, respectively.

**2.2. Dielectric Measurements.** Alternative current (ac) electric properties were analyzed from the capacitance and the dissipation factor values. An impedance analyzer (Wayne Kerr Electronics 65120B) was utilized in these measurements. The complex dielectric response was considered between 20 and 120 M Hz. In this study, the overall errors for the real and imaginary parts of the complex dielectric permittivity in the low- and high-frequency region were 2.5%. The root-mean-square (rms) amplitude of the device is ~453 mV.

### 3. THEORY

**3.1. Dielectric Properties.** The complex dielectric permittivity  $\epsilon$  is defined as  $\epsilon = \epsilon' + i\epsilon''$ . Here  $\epsilon'$  and  $\epsilon''$  are described as the real and imaginary parts of the complex dielectric permittivity. The complex conjugate of  $\epsilon$  is denoted as  $\epsilon^*$ , where  $\epsilon^* = \epsilon' - i\epsilon''$ . The product of a complex number

and its conjugate are real numbers  $\epsilon \times \epsilon^* = (\epsilon')^2 + (\epsilon'')^2$ . Therefore, the complex conjugate of the dielectric permittivity can be written as<sup>99–101</sup>

$$\epsilon^*(\omega) = \epsilon'(\omega) - i\epsilon''(\omega) = \epsilon_\infty + \frac{\epsilon_s - \epsilon_\infty}{1 + (i\omega\tau)^{1-\alpha}} \quad (1)$$

Here

$$\epsilon'(\omega) = \epsilon_s + (\epsilon_\infty - \epsilon_s) \times \frac{1 + (\omega\tau)^{1-\alpha} \sin\left(\frac{\pi\alpha}{2}\right)}{1 + 2 \sin\left(\frac{\pi\alpha}{2}\right)(\omega\tau)^{(1-\alpha)} + (\omega\tau)^{2(1-\alpha)}} \quad (2)$$

and

$$\epsilon''(\omega) = (\epsilon_\infty - \epsilon_s) \times \frac{(\omega\tau)^{1-\alpha} \sin\left(\frac{\pi\alpha}{2}\right)}{1 + 2 \sin\left(\frac{\pi\alpha}{2}\right)(\omega\tau)^{(1-\alpha)} + (\omega\tau)^{2(1-\alpha)}} \quad (3)$$

In this expression,  $\epsilon_\infty$  and  $\epsilon_s$  are high and static (low) frequency dielectric constants, respectively.  $\tau$  is the dielectric relaxation time. The parameter,  $\alpha$ , changes from zero to one ( $0 < \alpha \leq 1$ ), and this depends on temperature. If  $\alpha = 0$ , it corresponds to standard Debye-type relaxation.<sup>102</sup> The frequency evolution of the real ( $\epsilon'$ ) and imaginary part ( $\epsilon''$ ) of the dielectric constant

for MB-doped hydrogels was studied in the 10 Hz to 100 MHz frequency range. The parameter,  $\alpha$ , has values different from zero for all temperatures.

The complex dielectric constant  $\epsilon$  ( $\epsilon = \epsilon' + i\epsilon''$ ) is described by the Debye type ( $\alpha = 0$ ) equation

$$\epsilon(\omega) = \epsilon_{\infty} + \frac{\epsilon_s - \epsilon_{\infty}}{1 + i\omega\tau} \quad (4)$$

Here  $i$  and  $\omega$  are the imaginary number unit and the angular frequency, respectively. The real  $\epsilon'$  and the imaginary part  $\epsilon''$  of the complex dielectric constant are

$$\epsilon'(\omega) = \epsilon_{\infty} + \frac{\epsilon_s - \epsilon_{\infty}}{1 + i\omega^2\tau^2} \quad (5)$$

and

$$\epsilon''(\omega) = \frac{\omega\tau(\epsilon_s - \epsilon_{\infty})}{1 + i\omega^2\tau^2} \quad (6)$$

Thus, the relation between  $\epsilon'$  and  $\epsilon''$  can be describe by

$$\left( \epsilon'(\omega) - \left( \epsilon_{\infty} + \frac{\epsilon_s - \epsilon_{\infty}}{2} \right) \right)^2 + \epsilon''(\omega)^2 = \left( \frac{\epsilon_s - \epsilon_{\infty}}{2} \right)^2 \quad (7)$$

This equation related to circle.<sup>103</sup> The Cole–Cole plots are not seen in this work from the MB-doped hydrogels are ionic conductivity. This result suggests that the ionic conductivity originated from the MB doping.

**3.2. Impedance Properties.** Impedance measurement techniques were used to measure the response of the sample to the root-mean-square (rms) amplitude of the device response over the range of frequencies. The complex impedance of the sample is denoted by  $Z^*(\omega) = Z' + jZ'' = R + jX$ , where  $\omega$  is the angular frequency,  $Z(\omega)$  is the complex impedance,  $Z'$  is the real part,  $Z''$  is the imaginary part of the complex impedance,  $R$  is the resistance, and  $X$  is the reactance response to an alternating signal. The magnitude of the complex impedance,  $|Z^*(\omega)| = ((Z')^2 + (Z'')^2)^{1/2}$ , and the phase angle,  $\theta = \tan^{-1}(Z''/Z')$ , include the complex impedance.<sup>104–106</sup>

#### 4. RESULTS AND DISCUSSION

The frequency evolution of the real part ( $\epsilon'$ ), the imaginary part ( $\epsilon''$ ) of the complex dielectric constant, and the energy loss tangent/dissipation factor in the experimental results for hydrogels with different MB concentrations are shown in Figure 2.

The  $\epsilon'$  was recorded in the frequency range of 10 Hz to 100 MHz at RT in Figure 2a. The frequency evolutions of  $\epsilon'$  for hydrogels with different MB concentrations (25, 50, 75, 100 mg/L) are slowly decreasing, while the frequency is increasing. This low-frequency behavior for all hydrogels originates from the electrode polarization.<sup>59,89</sup> In addition, the  $\epsilon'$  for all samples decreases with the increase in the electrical conductivity.  $\epsilon'$  of the dielectric constant has decreased as the MB concentration decreases. The  $\epsilon'$  for all MB-doped hydrogels shows independent behavior above 10<sup>5</sup> Hz. The  $\epsilon'$  value for the 25 mg/L MB-doped hydrogel is also smaller than that of other samples above 10<sup>5</sup> Hz. The real  $\epsilon'$  increases as the MB concentration increases, but a completely opposite result was seen when the MB concentration was 75 mg/L. The  $\epsilon'$  strongly depends on the MB concentration of the hydrogels. In this

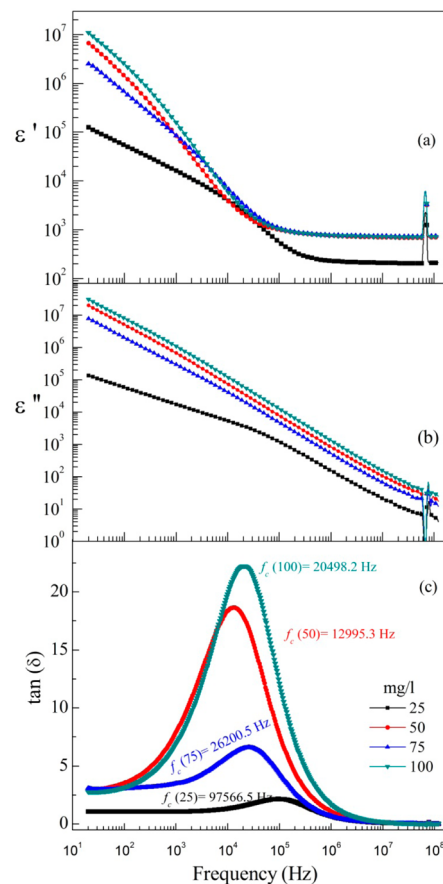


**Figure 2.** Frequency evolution of the real part (a), imaginary part (b) of the complex dielectric constant, and the energy loss tangent/dissipation factor (c) for hydrogels with different MB concentration, respectively.

work, this concentration value for hydrogels corresponds to the critical values.

It can be seen from Figure 2b that a linear decrease is present in  $\epsilon''$  with increasing frequency. The  $\epsilon''$  has been observed A a small peak near the 10<sup>5</sup> Hz for the 25 mg/L MB-doped hydrogels. This peak originates from the level of the energy loss of this hydrogels. This behavior was previously observed in our first study.<sup>2</sup> The  $\epsilon''$  of the dielectric permittivity has increased with the MB concentration increase. The relaxation times were measured by using the  $\epsilon''-f$  figures (Figure 2b). The MB concentration evolution of the imaginary  $\epsilon''$  has similar behavior as the real  $\epsilon'$ . The opposite result for the MB concentration evolution of the  $\epsilon''$  was seen when the MB concentration was increased to 75 mg/L.

Moreover, the energy or dielectric loss,  $\epsilon''$ , was calculated from eq 8

$$\text{dissipation factor; } \tan \delta = \frac{\epsilon''}{\epsilon'} \quad (8)$$

Here  $\delta = 90^\circ - \varphi$  and  $\varphi$  is the phase angle. The loss tangent ( $\tan \delta = \epsilon''/\epsilon'$ ) is also a typical consideration as a characteristic quantity of the dielectric. The frequency evolution of the energy loss factor ( $\tan \delta = \epsilon''/\epsilon'$ ) values of the samples are depicted in Figure 2c. The frequency decreases and the loss tangent value improves while the MB concentration increases. The minimum and maximum values of the energy loss factor for 25 and 100 mg/L MB-doped hydrogels are 2.19 and 22.13

respectively, but the loss tangent peak values for 50 and 75 mg/L MB-doped hydrogels cause the oscillation dependence on frequency. The maximum and minimum frequency values of 25 and 50 mg/L MB-doped hydrogels correspond to 97 566.5 and 12 995.3 Hz, respectively. The broadening of the maximum peak of the 100 mg/L MB-doped hydrogel is attributed to the change of the molecular vibration to rotational motion. The dissipation factor/tan  $\delta$  and maximum peak frequency values of the samples are listed in Table 1. The diameter and thickness of samples were measured by using a Mitutoyo micrometer.

**Table 1. Maximum Energy Loss Tangent/Dissipation Factor and Maximum Peak Frequency Values for Hydrogels with Different MB Concentrations**

sample	max. peak frequency (Hz)	max. peak tan $\delta$	diameter (mm)	thickness (mm)
25	97 566.5	2.19	2.69	4.85
50	12 995.3	18.64	3.94	1.51
75	26 200.5	6.57	3.49	1.41
100	20 498.2	22.13	4.28	1.52

The complex dielectric permittivity has been widely used to assess the electrode polarization and ionic conduction effects on doped hydrogels. The complex dielectric permittivity plane is plotted in two different arcs using the real  $\epsilon'$  and imaginary  $\epsilon''$  at RT in Figure 3. The electrode polarization results from

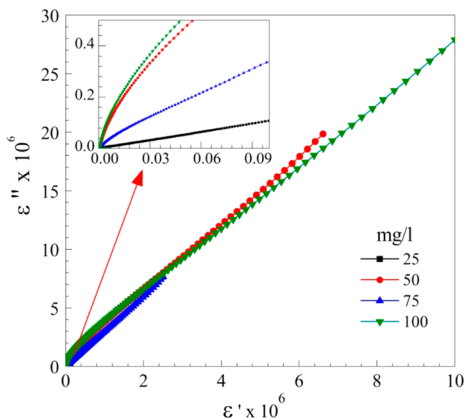


**Figure 3.** Complex dielectric plane plots for hydrogels with different MB concentrations.

the formation of electric double-layer capacitances with the free charge. These capacitances originate from the interface between the electrode surfaces and the dielectric materials in plane region. This phenomenon occurs by the substantial increase in the complex dielectric permittivity with the decreasing frequency in the lower frequency range of the electric signal.<sup>89,92</sup> Figure 3 shows the imaginary  $\epsilon''$  versus real  $\epsilon'$  plots for hydrogels with different MB concentration. The Cole–Cole plots of the imaginary  $\epsilon''$  and real part  $\epsilon'$  of the complex dielectric for pure/undoped hydrogels correspond to an equivalent electrical circuit (see ref 2 for detail), but this type of electrical circuit is not formed for hydrogels with an different MB concentration with an electric double layer (EDL) in this study.<sup>89</sup> In addition, the inset in Figure 3 shows the Cole–Cole plots of the imaginary  $\epsilon''$  and real part  $\epsilon'$  of the complex dielectric in detail at lower values.

Figure 4 shows the frequency evolution of the resistance–reactance values and the impedance ( $Z$ ) in log–log graph for

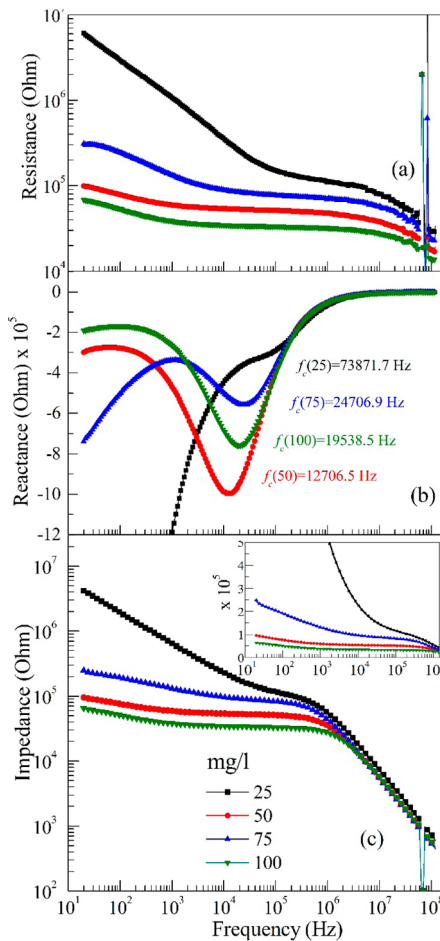


**Figure 4.** Frequency evolution of the resistance in log–log graph, the reactance, and the impedance ( $Z$ ) in log–log graph for different hydrogels with different MB concentrations.

hydrogels with different MB concentrations in the frequency range of 20 Hz to 120 MHz.

The experimental results of the resistance in Figure 4a are similar to the frequency evolution of impedance in Figure 4c. The resistance for MB-loaded hydrogels has nearly linear decreased with the frequency. This linear behavior sharply decreases for 25 mg/L MB-doped hydrogels below 10<sup>5</sup> Hz. The resistance values decrease with the increase in the rate of contribution of MB-doped hydrogels. In the low-frequency region, the largest value of the resistance was recorded for 25 mg/L, while its smallest value was observed for 100 mg/L MB-doped hydrogels. These results suggest that MB doping increased the conductivity if hydrogels. Similar resistance values were observed for all samples above 10<sup>7</sup> Hz frequency.

The frequency evolutions of reactance values for all MB-doped hydrogels are shown in Figure 4b. The reactance for 50, 75, and 100 mg/L MB-doped hydrogels present a minimum and then a maximum with the increasing frequency. Reactance values for all samples tend to zero in the high-frequency region. In this region, the reactance is proportional to the 1/frequency. The maximum and minimum reactance values correspond to 100 and 25 mg/L MB-doped hydrogels, respectively, in the low frequency. The critical frequencies for 25, 50, 75, and 100 mg/L

MB-doped hydrogels have been determined as 73871.7, 12706.5, 24706.9, and 19538.5 Hz, respectively. These frequency values have been shown in Table 2. The dielectric

**Table 2. Dielectric Parameters of MB-Doped Hydrogels**

sample	$\epsilon_s$	$\epsilon_\infty$	$\Delta\epsilon$	$f_c$ (Hz)
25	$0.124563 \times 10^6$	209.865	124353.135	73871.7
50	$6.61605 \times 10^6$	709.779	$6.61534 \times 10^6$	12706.5
75	$2.50542 \times 10^6$	757.361	$2.50466 \times 10^6$	24706.9
100	$1.10267 \times 10^6$	732.472	$1.1026 \times 10^6$	19538.5

relaxation strength  $\Delta\epsilon$  is the difference between the dielectric values at low and high frequencies. In the dielectric spectroscopy technique, the dielectric relaxation strength  $\Delta\epsilon$  is expressed as

$$\Delta\epsilon = \epsilon_s - \epsilon_\infty \quad (9)$$

where  $\epsilon_s$  and  $\epsilon_\infty$  are the low- and high-frequency components of the real part of dielectric constant.  $\epsilon_s$ ,  $\epsilon_\infty$ , and  $\Delta\epsilon$  values are given in the Table 2. The  $\epsilon_s$  and  $\epsilon_\infty$  values depend on temperature and doped concentration. In this study, the MB-doped hydrogels depend on the MB concentrations amount at RT. The concentrations evolutions of the  $\epsilon_s$  and  $\epsilon_\infty$  in this work are slowly increasing and decreasing, respectively. This finding confirms that the 50 and 75 mg/L MB doping causes critical changes to hydrogel's mechanical, thermal, and especially electrical conductivity properties without affecting the dielectric constant.

The reactance can be derived by solving the continuity equation/Poisson<sup>64</sup> for the potential across the MB-doped samples. The reactance values in the lower frequency side are in accordance with the contribution of the MB concentrations effect.

The frequency variation of the impedance ( $Z$ ) in log-log graph for hydrogels with different MB concentrations is given in Figure 4c. The semilog graph for hydrogels with different MB concentrations is depicted in the inset of Figure 4c. The impedance for 50, 75, and 100 mg/L MB-doped hydrogels has decreased logarithmically with the frequency. The impedance for 25 mg/L MB-doped sample is distinct from the others, as it decreased exponentially in the 10–10<sup>6</sup> Hz frequency range at RT. The impedance for all samples linearly decreases above 10<sup>6</sup> Hz frequency. This linear behavior in the frequency range of 10<sup>6</sup>–10<sup>8</sup> Hz originates from the inductance effects. An alternative explanation is that the capacitance effects have been activated below 10<sup>6</sup> Hz frequency. In the lower frequency region, the largest value of the impedance was observed for 25 mg/L MB-doped hydrogels, while its smallest value was recorded for 100 mg/L MB-doped hydrogels.

The MB concentration effect of MB doping of hydrogels on the phase angle in the frequency range of 10 Hz to 100 MHz is shown in Figure 5. The concentration effect results indicate that the phase angles of 50, 75, and 100 mg/L MB-doped hydrogels exhibit similar behavior. The 25 mg/L MB-doped sample exhibits a different phase angle change trend compared with the other samples, especially at the low-frequency region. The phase angle values for 50–100 mg/L MB-doped hydrogels are 20 and ~42° near the 10 Hz, respectively. The lowest value of the phase angle for 100 mg/L MB-doped sample was measured as 4° near the 10<sup>4</sup> Hz, while this value for 25 mg/L MB-doped sample was observed as ~25°. However, there is some anomaly at 10<sup>3</sup> Hz frequency, and this anomaly originates from the

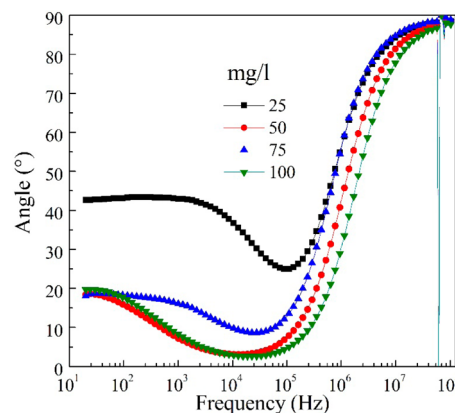


**Figure 5.** Frequency variation of the phase angle for hydrogels with different MB concentrations.

viscoelastic characteristics. Near the 10<sup>8</sup> Hz frequency, the phase angles are 90° for all samples. This result is compatible with the  $\delta = 90^\circ - \varphi$ .

## 5. CONCLUSIONS

The frequency evolution of real part ( $\epsilon'$ ) and the imaginary part ( $\epsilon''$ ) of dielectric permittivity and the energy loss tangent/dissipation factor ( $\tan \delta$ ) for hydrogels with different MB concentrations have been investigated using the IS at RT. The complex dielectric permittivity plane is observed in the two different arcs using the real  $\epsilon'$  and the imaginary  $\epsilon''$  at RT for pH 5.5. In addition, frequency variations of the resistance, the reactance, and the impedance have been investigated for MB-doped hydrogels. As the amount of the contribution of MB increase, the real and imaginary parts of the complex dielectric constant increase in lower frequency region. Also, the maximum peak values of energy loss factor for MB-doped hydrogels increase with the increasing MB concentration in the 10<sup>3</sup>–10<sup>5</sup> Hz frequency range. The resistance, reactance, and impedance values sharply decrease with the increasing MB concentrations at lower frequencies. Nevertheless, completely opposite results were obtained when the MB concentrations was between 50 and 75 mg/L. This opposite behavior has been recorded for all of the samples in this study. This behavior originated from the strong dependence on the MB concentrations in hydrogels. It is anticipated that this fact is due to the common motion of MB–water molecules through hydrogen bonds.

The 3D matrices for hydrogels are made of covalent, ionic, van der Waals, and hydrogen bonds. The hydrogel structure depends on the method of preparation and method of cross-linking. The critical frequency values slip to the low-frequency region with the amount of the contribution of MB in this work. The critical frequency values for Cu-ion doped hydrogels are smaller than those of pure samples.<sup>2</sup> Moreover, the critical frequency for MB-doped samples is less than Cu-ion doped and pure samples. The impedance of MB-doped hydrogels decreases as the ionic conductivity increases, compared with the pure hydrogels. The dielectric permittivity of the MB-doped hydrogels is sensitive to ionic conduction and electrode polarization in low frequency. The frequency evolution of the ac conductivity obeys Jonscher power law in the high-frequency region. Furthermore, the dielectric behavior in high-frequency parts was attributed to the Brownian motion of the hydrogen

bonds. This result suggests that the non-Newtonian properties of MB-doped hydrogels may be studied by the IS technique.<sup>77</sup>

In conclusion, the ionic conduction and electrode polarization behaviors at lower frequencies and the Brownian motion at high frequencies have been identified for MB-doped hydrogels at RT. The Cole–Cole plots were not observed for MB-doped samples, while semicircle plots were obtained for pure samples.<sup>2</sup> The Cole–Cole plots for pure sample show equivalent electrical circuit. The ionic conduction for MB-doped samples was prevented for Cole–Cole plots. The ac conductivity increases with the increasing frequency and the MB concentration.<sup>86,88</sup>

## AUTHOR INFORMATION

### Corresponding Author

\*E-mail: o.yalcin@nigde.edu.tr or orhanyalcin@gmail.com. Tel: + 90 388 225 4068. Fax: +90 388 2250180.

### Notes

The authors declare no competing financial interest.

## REFERENCES

- (1) Peppas, N. A.; Mikos, A. G. Preparation Methods and Structure of Hydrogels. In *Hydrogels in Medicine and Pharmacy*; CRC Press: Boca Raton, FL, 1986; Vol. 1, pp 1–25.
- (2) Coşkun, R.; Okutan, M.; Yalçın, O.; Kösemen, A. Electric and Magnetic Properties of Hydrogels Doped with Cu Ions. *Acta Phys. Pol. A* **2012**, *122*, 683–687.
- (3) Qiu, Y.; Park, K. Environment-Sensitive Hydrogels for Drug Delivery. *Adv. Drug Delivery Rev.* **2012**, *64*, 49–60.
- (4) Buenger, D.; Topuz, F.; Groll, J. Hydrogels in Sensing Applications. *Prog. Polym. Sci.* **2012**, *37*, 1678–1719.
- (5) Liu, M.; Su, H.; Tan, T. Synthesis and Properties of Thermo- and pH-Sensitive Poly(N-isopropylacrylamide)/Polyaspartic Acid IPN Hydrogels. *Carbohydr. Polym.* **2012**, *87*, 2425–2431.
- (6) Mocanu, G.; Souguir, Z.; Picton, L.; Cerf, D. L. Multi-Responsive Carboxymethyl Polysaccharide Crosslinked Hydrogels Containing Jeffamine Side-Chains. *Carbohydr. Polym.* **2012**, *89*, 578–585.
- (7) Depa, K.; Strachota, A.; Šlouf, M.; Hromádková, J. Fast Temperature-Responsive Nanocomposite PNIPAM Hydrogels with Controlled Pore Wall Thickness: Force and Rate of T-Response. *Eur. Polym. J.* **2012**, *48*, 1997–2007.
- (8) Sun, X.; Wanga, H.; Jing, Z.; Mohanathas, R. Hemicellulose-Based pH-Sensitive and Biodegradable Hydrogel for Controlled Drug Delivery. *Carbohydr. Polym.* **2013**, *92*, 1357–1366.
- (9) Kurnia, J. C.; Birgersson, E.; Mujumdar, A. S. Analysis of a Model for pH-Sensitive Hydrogels. *Polymer* **2012**, *53*, 613–622.
- (10) Vashist, A.; Gupta, Y. K.; Ahmad, S. Interpenetrating Biopolymer Network Based Hydrogels for an Effective Drug Delivery System. *Carbohydr. Polym.* **2012**, *87*, 1433–1439.
- (11) Abd El-Ghaffar, M. A.; Hashem, M. S.; El-Awady, M. K.; Rabie, A. M. pH-Sensitive Sodium Alginate Hydrogels for Riboflavin Controlled Release. *Carbohydr. Polym.* **2012**, *89*, 667–675.
- (12) Wang, Y.; Dong, A.; Yuan, Z.; Chen, D. Fabrication and Characterization of Temperature-, pH- and Magnetic-Field-Sensitive Organic/Inorganic Hybrid Poly(ethylene glycol)-based Hydrogels. *Colloids Surf., A* **2012**, *415*, 68–76.
- (13) Wenceslau, A. C.; Santos, F. G.; Ramos, É. R. F.; Nakamura, C. V.; Rubira, A. F.; Muniz, E. C. Thermo- and pH-Sensitive IPN Hydrogels Based on PNIPAAm and PVA-Ma Networks with LCST Tailored Close to Human Body Temperature. *Mater. Sci. Eng., C* **2012**, *32*, 1259–1265.
- (14) Anderson, J. M.; Allen, J. M. J.; Dempsey, G. J. *Sensor Device*. U.S. Patent 6055448, 2000.
- (15) Wichterle, O.; Lim, D. Hydrophilic Gels for Biological Use. *Nature* **1960**, *185*, 117–118.
- (16) Abd El-Rehim, H. A.; Hegazy, E. A.; Abd El-Mohdy, H. L. Radiation Synthesis of Hydrogels to Enhance Sandy Soils Water Retention and Increase Plant Performance. *J. Appl. Polym. Sci.* **2004**, *93*, 1360–1371.
- (17) Chow, E.; Lin, S. Y.; Johnson, S. G.; Villeneuve, P. B.; Joannopoulos, J. D.; Wendt, J. R.; Vawter, G. A.; Zubrzycki, W.; Hou, H.; Alleman, A. Three-Dimensional Control of Light in a Two-Dimensional Photonic Crystal Slab. *Nature* **2000**, *407*, 983–986.
- (18) Sow, C. H.; Bettoli, A. A.; Lee, Y. Y. G.; Cheong, F. C.; Lim, C. T.; Watt, F. Multiple-Spot Optical Tweezers Created with Microlens Arrays Fabricated by Proton Beam Writing. *Appl. Phys. B: Lasers Opt.* **2004**, *78*, 705.
- (19) Langer, R. Drugs on Target. *Science* **2001**, *293*, 58–59.
- (20) Soussan, E.; Cassel, S.; Blanzat, M. Drug Delivery by Soft Matter: Matrix and Vesicular Carriers. *Angew. Chem., Int. Ed.* **2009**, *48*, 274–288.
- (21) Nanjawade, B. K.; Manvi, F. V.; Manjappa, A. S. In Situ-Forming Hydrogels for Sustained Ophthalmic Drug Delivery. *J. Controlled Release* **2007**, *122*, 119–134.
- (22) Missirlis, D.; Tirelli, N.; Hubbell, J. A. Amphiphilic Hydrogel Nanoparticles. Preparation, Characterization, and Preliminary Assessment as New Colloidal Drug Carriers. *Langmuir* **2005**, *21*, 2605–2613.
- (23) Crescenzi, V.; Cornelio, L.; Meo, C. D.; Nardeccchia, S.; Lamanna, R. Novel Hydrogels via Click Chemistry: Synthesis and Potential Biomedical Applications. *Biomacromolecules* **2007**, *8*, 1844–1850.
- (24) Golden, A. P.; Tien, J. Fabrication of Microfluidic Hydrogels Using Molded Gelatin as a Sacrificial Element. *Lab Chip* **2007**, *17*, 720–725.
- (25) Abd El-Mohdy, H. L.; Hegazy, E. A.; El-Nesr, E. M.; El-Wahab, M. A. Synthesis, Characterization and Properties of Radiation-Induced Starch/(EG-co-MAA) Hydrogels. *Arabian J. Chem.* **2012**, *1*–9.
- (26) Nishikawa, T.; Akiyoshi, K.; Sunamoto, J. Supramolecular Assembly between Nanoparticles of Hydrophobized Polysaccharide and Soluble Protein Complexation between the Self-Aggregate of Cholesterol-Bearing Pullulan and  $\alpha$ -Chymotrypsin. *Macromolecules* **1994**, *27*, 7654–7659.
- (27) Hoare, T. R.; Kohane, D. S. Hydrogels in Drug Delivery: Progress and Challenges. *Polymer* **2008**, *49*, 1993–2007.
- (28) Coville, T.; Matricardi, P.; Marianetti, C.; Alhague, F. Polysaccharide Hydrogels for Modified Release Formulations. *J. Controlled Release* **2007**, *119*, 5–24.
- (29) Peppas, N. A.; Bures, P.; Leobandung, W.; Ichikawa, H. Hydrogels in Pharmaceutical formulations. *Eur. J. Pharm. Biopharm.* **2000**, *50*, 27–46.
- (30) Wheeldon, I.; Ahari, A. F.; Khademhosseini, A. Microengineering Hydrogels for Stem Cell Bioengineering and Tissue Regeneration. *JALA* **2010**, *3*, 1–9.
- (31) Slaughter, B. V.; Khurshid, S. S.; Fisher, O. Z.; Khademhosseini, A.; Peppas, N. A. Hydrogels in Regenerative Medicine. *Adv. Mater.* **2009**, *21*, 3307–3329.
- (32) Peppas, N. A.; Bures, P.; Leobandung, W.; Ichikawa, H. Hydrogels in Pharmaceutical Formulations. *Eur. J. Pharm. Biopharm.* **2000**, *50*, 27–46.
- (33) Hoffman, A. S. Hydrogels for Biomedical Applications. *Adv. Drug Delivery Rev.* **2002**, *54*, 3–12.
- (34) Chen, X.; Martin, B. D.; Neubauer, T. K.; Linhardt, R. J.; Dordick, J. S.; Rethwisch, D. G. Enzymatic and Chemoenzymatic Approaches to Synthesis of Sugar-Based Polymer and Hydrogels. *Carbohydr. Polym.* **1995**, *28*, 15–21.
- (35) Ajji, Z.; Othman, I.; Rosiak, J. M. Production of Hydrogel Wound Dressings Using Gamma Radiation. *Nucl. Instrum. Methods Phys. Res., Sect. B* **2005**, *229*, 375–380.
- (36) Hoare, T. R.; Kohane, D. S. Hydrogels in Drug Delivery: Progress and Challenges. *Polymer* **2008**, *49*, 1993–2007.
- (37) Benamer, S.; Mahlous, M.; Boukrif, A.; Mansouri, B.; Youcef, S. L. Synthesis and Characterisation of Hydrogels Based on Poly(vinyl pyrrolidone). *Nucl. Instrum. Methods Phys. Res., Sect. B* **2006**, *248*, 284–290.
- (38) Nho, Y.-C.; Park, S. E.; Kim, H. I.; Hwang, T. S. Oral Delivery of Insulin Using pH Sensitive Hydrogels Based on Polyvinyl Alcohol

- Grafted with Acrylic Acid/Methacrylic Acid by Radiation. *Nucl. Instrum. Methods Phys. Res., Sect. B* **2005**, *236*, 283–288.
- (39) Ajji, Z. Preparation of Poly(vinyl alcohol) Hydrogels Containing Citric or Succinic Acid Using Gamma Radiation. *Radiat. Phys. Chem.* **2005**, *74*, 36–41.
- (40) Şahiner, N.; Malci, S.; Çelikbıçak, Ö.; Kantoğlu, Ö.; Salih, B. Radiation Synthesis and Characterization of New Hydrogels Based on Acrylamide Copolymers Cross-Linked with 1-Allyl-2-thiourea. *Radiat. Phys. Chem.* **2005**, *74*, 76–85.
- (41) Francis, S.; Varshney, L. Studies on Radiation Synthesis of PVA/EDTA Hydrogels. *Radiat. Phys. Chem.* **2005**, *74*, 310–316.
- (42) Ali, A. E.; Shawky, H. A.; Abd El Rehim, H. A.; Hegazy, E. A. Synthesis and Characterization of PVP/Acrylic Acid Copolymer Hydrogel and Its Applications in the Removal of Heavy Metals from Aqueous Solution. *Eur. Polym. J.* **2003**, *39*, 2337–2344.
- (43) Abd Alla, S. G.; El-Din, H. M. N.; El-Naggar, A. W. M. Structure and Swelling-Release Behaviour of Poly(vinyl pyrrolidone) (PVP) and Acrylic Acid (AAc) Copolymer Hydrogels Prepared by Gamma Irradiation. *Eur. Polym. J.* **2007**, *43*, 2987–2998.
- (44) Karadag, E.; Üzüm, Ö. B.; Saraydin, D.; Güven, O. Swelling Characterization of Gamma-Radiation Induced Crosslinked Acrylamide/Maleic Acid Hydrogels in Urea Solutions. *Mater. Des.* **2006**, *27*, 576–584.
- (45) Wang, W.; Wang, J.; Kang, Y.; Wang, A. Synthesis, Swelling and Responsive Properties of a New Composite Hydrogel Based on Hydroxyethyl Cellulose and Medicinal Stone. *Composites, Part B* **2011**, *42*, 809–818.
- (46) Rivest, C.; Morrison, D. W. G.; Ni, B.; Rubin, J.; Yadav, V.; Mahdavi, A.; Karp, J. M.; Khademhosseini, A. Microscale Hydrogels for Medicine and Biology: Synthesis, Characteristics and Applications. *Mech. Adv. Mater. Struct.* **2007**, *2*, 1103–1119.
- (47) Ahearne, M.; Yang, Y.; Liu, K.-K. Mechanical Characterisation of Hydrogels for Tissue Engineering Applications. *Top. Tissue Eng.* **2008**, *4*, 1–16.
- (48) Tsuchida, E.; Nishide, H. Polymer-Metal Complexes and Their Catalytic Activity. *Adv. Polym. Sci.* **1977**, *24*, 1–87.
- (49) Higashi, F.; Chong, C. S.; Kakinoki, H.; Sumita, O. A New Organic Semiconducting Polymer from Cu<sup>2+</sup> Chelate of Poly(vinyl alcohol) and Iodine. *J. Polym. Sci., Polym. Chem.* **1979**, *17*, 313–318.
- (50) Buchmeiser, M. R.; Kröll, R.; Wurst, K.; Schareina, T.; Kempe, R. Polymer-Supported Polymerization Catalysts via ROMP. *Macromol. Symp.* **2001**, *164*, 187–196.
- (51) Michalska, Z. M.; Strzelec, K.; Sobczak, J. W. Hydrosilylation of Phenylacetylene Catalyzed by Metal Complex Catalysts Supported on Polyamides Containing a Pyridine Moiety. *J. Mol. Catal. A: Chem.* **2000**, *156*, 91–102.
- (52) Akelah, A.; Moet, A. *Functionalised Polymers and Their Applications*; Chapman and Hall: London, 1990; Vol.30, p 354.
- (53) Okutan, M.; Şentürk, E. Dielectric Relaxation Mode in Side-Chain Liquid Crystalline Polymer Film. *J. Non-Cryst. Solids.* **2008**, *354*, 1526–1530.
- (54) Şentürk, E.; Okutan, M.; San, S. E.; Köysal, O. Debye Type Dielectric Relaxation in Carbon Nano-Balls' and 4-DMAABCA Acid Doped E7 Coded Nematic Liquid Crystal. *J. Non-Cryst. Solids* **2008**, *354*, 3525–3528.
- (55) Peppas, N. A. Physiologically Responsive Hydrogels. *J. Biact. Compat. Polym.* **1991**, *6*, 241–246.
- (56) Peppas, N. A. Fundamentals of pH- and Temperature Sensitive Delivery Systems. In *Pulsatile Drug Delivery*; Wissenschaftliche Verlagsgesellschaft: Stuttgart, Germany, 1993; Vol. 51, pp 41–56.
- (57) Rosiak, J. M.; Yoshii, F. Hydrogels and Their Medical Applications. *Nucl. Instrum. Methods Phys. Res., Sect. B* **1999**, *151*, 56–64.
- (58) Hennink, W. E.; Nostrum, C. F. Novel Crosslinking Methods to Design Hydrogels. *Adv. Drug Delivery Rev.* **2002**, *54*, 13–36.
- (59) Masci, G.; Cametti, C. Dielectric Properties of Thermo-Reversible Hydrogels: The Case of a Dextran Copolymer Grafted with Poly(*N*-isopropylacrylamide). *J. Phys. Chem. B* **2009**, *113*, 11421–1428.
- (60) Yang, L. J.; Yang, X. Q.; Huang, K. M.; Jia, G. Z.; Shang, H. Dielectric Properties of Binary Solvent Mixtures of Dimethyl Sulfoxide with Water. *Int. J. Mol. Sci.* **2009**, *10*, 1261–1270.
- (61) Hill, N. E. *Dielectric Properties and Molecular Behaviour*; Van Nostrand Reinhold: New York, 1969.
- (62) Murthi, Y. V. G. S.; Prasad, P. S. Dielectric Loss and Electrical-Conductivity Studies on Copper-Doped NH<sub>4</sub>Cl Crystals. *Physica* **1974**, *77*, 543–556.
- (63) Smyth, C. P. *Dielectric Behavior and Structure Phelps*; McGraw-Hill Book Company: New York, 1955; Vol. 11, p 441.
- (64) Barbero, G.; Alexe-Ionescu, A. L.; Lelidis, I. Significance of Small Voltage in Impedance Spectroscopy Measurements on Electrolytic Cells. *J. Appl. Phys.* **2005**, *98*, 05202–5.
- (65) Pissis, P.; Kyritsis, A.; Konsta, A. A.; Daoukaki, D. Dielectric Studies of Molecular Mobility in Hydrogels. *J. Mol. Struct.* **1999**, *479*, 163–175.
- (66) Yeow, Y. K.; Abbas, Z.; Khalid, K.; Rahman, M. Z. A. Improved Dielectric Model for Polyvinyl Alcohol-Water Hydrogel at Microwave Frequencies. *Am. J. Appl. Sci.* **2010**, *7*, 270–276.
- (67) Kirker, K. R.; Prestwich, G. D. Physical Properties of Glycosaminoglycan Hydrogels. *Polym. Phys.* **2004**, *42*, 4344–4356.
- (68) Stammen, J. A.; Williams, S.; Ku, D. N.; Guldberg, R. E. Mechanical Properties of a Novel PVA hydrogel in Shear and Unconfined Compression. *Biomaterials* **2001**, *22*, 799–806.
- (69) Johnson, B.; Niedermaier, D. J.; Crone, W. C.; Moorthy, J.; Beebe, D. J. Mechanical Properties of a pH Sensitive Hydrogel. *Proc. SEM Conf. Exp. Mech.* **2002**, *45*, 1–4.
- (70) Pissis, P.; Kyritsis, A. Electrical Conductivity Studies in Hydrogels. *Solid State Ionics* **1997**, *97*, 105–113.
- (71) Gómez-Galván, F.; Ceniceros, T. L.; Mercado-Uribe, H. Device for Simultaneous Measurements of the Optical and Dielectric Properties of Hydrogels. *Meas. Sci. Technol.* **2012**, *23*, 025602-1–025602-6.
- (72) Bajpai, A. K.; Bajpai, J.; Soni, S. N. Preparation and Characterization of Electrically Conductive Composites of Poly(vinyl alcohol)-g-poly(acrylic acid) Hydrogels Impregnated with Polyaniline (PANI). *eXPRESS Polym. Lett.* **2008**, *2*, 26–39.
- (73) Kaur, N.; Singh, M.; Singh, A.; Awasthi, A. M.; Singh, L. Dielectric Relaxation Spectroscopy of Phlogopite Mica. *Physica B* **2012**, *407*, 4489–4494.
- (74) Kim, D.-H.; Abidian, M.; Martin, D. C. Conducting Polymers Grown in Hydrogel Scaffolds Coated on Neural Prosthetic Devices. *J. Biomed. Mater. Res., Part A* **2004**, *34*, 577–585.
- (75) Gabai, R.; Sallacan, N.; Chegel, V.; Bourenko, T.; Katz, E.; Willner, I. Characterization of the Swelling of Acrylamidophenylboronic Acid-Acrylamide Hydrogels upon Interaction with Glucose by Faradaic Impedance Spectroscopy, Chronopotentiometry, Quartz-Crystal Microbalance (QCM), and Surface Plasmon Resonance (SPR) Experiments. *J. Phys. Chem. B* **2001**, *105*, 8196–8202.
- (76) Pan, Y.; Xiong, D.; Gao, F. Viscoelastic Behavior of Nano-Hydroxyapatite Reinforced Poly(vinyl alcohol) Gel Biocomposites As an Articular Cartilage. *J. Mater. Sci: Mater. Med.* **2008**, *19*, 1963–1969.
- (77) Alexe-Ionescu, A. L.; Barbero, G.; Meyer, C. Influence of the Rheological Properties on the Electrical Impedance of Hydrogels. *J. Appl. Phys.* **2012**, *111*, 014905-1–014905-5.
- (78) Freire, F. C. M.; Becchi, M.; Ponti, S.; Miraldi, E.; Strigazzi, A. Impedance Spectroscopy of Conductive Commercial Hydrogels for Electromyography and Electroencephalography. *Physiol. Meas.* **2010**, *31*, S157–S169.
- (79) Huang, M.; Shen, D.; Chow, L. M.; Yang, M. Correlations of the Impedance Parameters and Conductivity and Permittivity of Liquid and Gel Phases in a Series Piezoelectric Quartz Crystal Sensor. *Sens. Actuators, B* **2001**, *72*, 21–27.
- (80) Pittini, Y. Y.; Daneshvari, D.; Pittini, R.; Vaucher, S.; Rohr, L.; Leparoux, S.; Leuenberger, H. Cole–Cole Plot Analysis of Dielectric Behavior of Monoalkyl Ethers of Polyethylene Glycol (C<sub>n</sub>E<sub>m</sub>). *Eur. Polym. J.* **2008**, *44*, 1191–1199.

- (81) Woerly, S.; Pinet, E.; de Robertis, L.; Van Diep, D.; Bousmina, M. Spinal Cord Repair with PHPMA Hydrogel Containing RGD Peptides (NeuroGel<sup>TM</sup>). *Biomaterials* **2001**, *22*, 1095–1111.
- (82) Richardson-Burns, S. M.; Hendricks, J. L.; Foster, B.; Povlich, L. K.; Kim, D.-H.; Martin, D. C. Polymerization of the Conducting Polymer Poly(3,4-ethylenedioxothiophene) (PEDOT) around Living Neural Cells. *Biomaterials* **2007**, *28*, 1539–1552.
- (83) He, L.; Lin, D.; Wang, Y.; Xiao, Y.; Che, J. Electroactive SWNT/PEGDA Hybrid Hydrogel Coating for Bio-Electrode Interface. *Colloids Surf., B* **2011**, *87*, 273–279.
- (84) Talary, M. S.; Dewarrat, F.; Caduff, A.; Puzenko, A.; Ryabov, Y.; Feldman, Y. An RCL Sensor for Measuring Dielectrically Lossy Materials in the MHz Frequency Range. Comparison of Hydrogel Model Simulation with Actual Hydrogel Impedance Measurements. *IEEE Trans. Dielectr. Insul.* **2006**, *13*, 247–256.
- (85) Xu, Y.; Huang, X.; Lin, Z.; Zhong, X.; Huang, Y.; Duan, X. One-Step Strategy to Graphene/Ni(OH)<sub>2</sub> Composite Hydrogels As Advanced 3D Supercapacitor Electrode Materials. *Nano Res.* **2012**, *11*, 1–14.
- (86) Sengwa, R. J.; Sankhla, S. Dielectric Dispersion Study of Coexisting Phases of Aqueous Polymeric Solution: Poly(vinyl alcohol) + Poly(vinyl pyrrolidone) Two-Phase Systems. *Polymer* **2007**, *48*, 2737–2744.
- (87) Sengwa, R. J.; Sankhla, S. Solvent Effects on the Dielectric Dispersion of Poly(vinyl pyrrolidone)-Poly(ethylene glycol) Blends. *Colloid Polym. Sci.* **2007**, *285*, 1237–1246.
- (88) Aziz, S. B.; Abidin, Z. H. Z.; Arof, A. K. Influence of Silver Ion Reduction on Electrical Modulus Parameters of Solid Polymer Electrolyte Based on Chitosan-Silver Triflate Electrolyte Membrane. *eXPRESS Polym. Lett.* **2010**, *4*, 300–310.
- (89) Sengwa, R. J.; Choudhary, S. Investigation of Correlation between Dielectric Parameters and Nanostructures in Aqueous Solution Grown Poly(vinyl alcohol)-Montmorillonite Clay Nanocomposites by Dielectric Relaxation Spectroscopy. *eXPRESS Polym. Lett.* **2010**, *4*, 559–569.
- (90) Pradhan, D. K.; Choudhary, R. N. P.; Samantaray, B. K. Studies of Structural, Thermal and Electrical Behavior of Polymer Nanocomposite Electrolytes. *eXPRESS Polym. Lett.* **2008**, *2*, 630–638.
- (91) Wang, M.; Dong, S. Enhanced Electrochemical Properties of Nanocomposite Polymer Electrolyte Based on Copolymer with Exfoliated Clays. *J. Power Sources* **2007**, *170*, 425–432.
- (92) Pandey, P. K.; Smitha, P.; Gajbhiye, N. S. Synthesis and Characterization of Nanostructured PZT Encapsulated PVA-PAA Hydrogel. *J. Polym. Res.* **2008**, *15*, 397–402.
- (93) Bordi, F.; Cametti, C.; Paradossi, G. Radiowave Dielectric Properties of Xanthan in Aqueous Solutions. *J. Phys. Chem.* **1995**, *99*, 274–284.
- (94) Bordi, F.; Cametti, C.; Colby, R. H. Dielectric Spectroscopy and Conductivity of Polyelectrolyte Solutions. *J. Phys.: Condens. Matter* **2004**, *16*, R1423–R1463.
- (95) Bordi, F.; Cametti, C.; Motta, A.; Paradossi, G. Electrical Conductivity of Dilute and Semidilute Aqueous Polyelectrolyte Solutions. A Scaling Theory Approach. *J. Phys. Chem. B* **1999**, *103*, 5092–5099.
- (96) Bordi, F.; Cametti, C.; Gili, T. Reduction of the Contribution of Electrode Polarization Effects in the Radiowave Dielectric Measurements of Highly Conductive Biological Cell Suspensions. *Bioelectrochemistry* **2001**, *54*, 53–61.
- (97) Coşkun, R.; Delibaş, A. Removal of Methylene Blue from Aqueous Solutions by Poly(2-acrylamido-2-methylpropane sulfonic acid-co-itaconic acid) Hydrogels. *Polym. Bull.* **2012**, *68*, 1889–1903.
- (98) Coşkun, R. Removal of Cationic Dye from Aqueous Solution by Adsorption onto Crosslinked Poly(4-vinylpyridine/crotonic acid) and Its N-Oxide Derivative. *Polym. Bull.* **2011**, *67*, 125–140.
- (99) Cho, M. S.; Cho, Y. H.; Choi, H. J.; Jhon, M. S. Synthesis and Electrorheological Characteristics of Polyaniline-coated PMMA Microsphere: Size Effect. *Langmuir* **2003**, *19*, 5875–5881.
- (100) Scaife, B. K. P. *Principles of Dielectrics*; Clarendon Press: Oxford, U. K., 1989; Vol.4S, p 448.
- (101) Cho, Y. H.; Cho, M. S.; Choi, H. J.; Jhon, M. S. Electrorheological Characterization of Polyaniline-coated Poly(methyl methacrylate) Suspensions. *Colloid Polym. Sci.* **2002**, *280*, 1062–1066.
- (102) Wang, L.-M.; Richert, R. Debye Type Dielectric Relaxation and the Glass Transition of Alcohols. *J. Phys. Chem. B* **2005**, *109*, 11091–11094-4.
- (103) Cole, K. S.; Cole, R. H. Dispersion and Absorption in Dielectrics - I Alternating Current Characteristics. *J. Chem. Phys.* **1941**, *9*, 341–352.
- (104) Pradhan, D. K.; Samantaray, B. K.; Choudhary, R. N. P.; Thakur, A. K. Complex Impedance Studies on a Layered Perovskite Ceramic Oxide—NaNdTiO<sub>4</sub>. *Mater. Sci. Eng., B* **2005**, *116*, 7–13.
- (105) Macdonald, J. R. *Impedance Spectroscopy: Emphasizing Solid Materials and Systems*; Wiley, New York, 1987.
- (106) El-Gendy, Y. A.; Yahia, I. S.; Yakuphanoglu, F. Investigation of Nanocrystalline CdS/Si Diode Using Complex Impedance Spectroscopy. *Mater. Res. Bull.* **2012**, *47*, 3397–3402.